

Quantum Confinement in PbI₂ Nanodisks Prepared with Cucurbit[7]uril

Erick M. S. dos Santos, Lourivaldo S. Pereira and Grégoire J.-F. Demets*

DQ-FFCLRP, Departamento de Química, Universidade de São Paulo, 14040-901 Ribeirão Preto-SP, Brazil

Este trabalho apresenta uma rota alternativa para a preparação de nanodiscos de iodeto de chumbo (*ca.* 50-340 × 7 Å, diâmetro × espessura) utilizando o macrocíclico cucurbit[7]urila como molde de síntese e agente estabilizante. Estas nanopartículas apresentam um deslocamento para o azul de *gap* óptico consistente com seu tamanho reduzido e confinamento quântico 1D. Suas espessuras são compatíveis com a de uma camada de iodeto de chumbo esfoliado, indicando que cucurbit[7]urila impede a formação de estruturas lamelares e limita o crescimento das nanopartículas. A estrutura, a morfologia e as propriedades destes discos foram verificadas por difratometria de raios X em pó (XRD), espectroscopia no UV-Visível, microscopia de força atômica (AFM), microscopia eletrônica de varredura com análise de fluorescência de raios X por dispersão de energia (SEM-EDS) e microscopia eletrônica de transmissão de alta resolução (HRTEM).

This work presents an alternative route for the preparation of heavy metal iodide nanoparticles, particularly lead iodide nanodisks (*ca.* 50-340 × 7 Å, diameter × thickness), using the macrocycle cucurbit[7]uril as a synthetic template and stabilizing agent. These nanoparticles exhibit an optical-gap blue shift consistent with their small size and 1D quantum confinement. Their thicknesses are compatible with an exfoliated single layer of lead iodide, indicating that cucurbit[7]uril, preventing the stacking and formation of tactoids, thus limiting nanoparticles growth in the z direction. The structure, morphology and properties of these disks were analyzed by X-ray powder diffractometry (XRD), UV-Visible spectroscopy, atomic force microscopy (AFM), scanning electron microscopy with analysis of energy dispersive X-ray fluorescence (SEM-EDS) and high resolution transmission electron microscopy (HRTEM).

Keywords: lead iodide, cucurbit[7]uril, synthetic template, nanodisks, quantum confinement

Introduction

Lead iodide is a lamellar solid consisting of layers of metal and iodide ions united by covalent bonds. Weak van der Waals interactions hold these layers together in a three dimensional sandwich-like semiconductor. This structure can be described as a hexagonal close-packed array of iodide anions with alternate layers of octahedral interstices occupied by lead(II) cations. Therefore, each layer can be described as a I-Pb-I sequence layer.¹ Very interesting materials can be obtained by diminishing the PbI₂ particle size to the nanoscale in order to favor the appearance of new properties resultant of quantum confinement, such as those observed in zero-dimensional solids, quantum dots and other N-dimensional, quantum-confined nanomaterials. Quantum dots encounter many applications in several technological fields such as sensor

devices and anti-counterfeiting systems, illumination (as high efficiency white-light emitting diodes), medicine (as cellular markers), lasers, solar cells and others.²⁻⁵ Another important property of lead iodide is its ability to form intercalation compounds with many chemical species, such as hydrazine, ammonia, aniline, butylamine, piperidine and quinoline, among others.¹ The insertion of guest molecules in the interlamellar gap considerably affects the chemical and physical properties of the material.

Cucurbiturils (CB[n]) are pumpkin-shaped thoroidal molecules with two distal portals separated by 9.1 Å. They are produced by condensation of glycoluril and formaldehyde in acidic medium and were synthesized for the first time by Behrend *et al.* in 1905.⁶ However, their structure remained uncertain until the findings of Freeman *et al.*, 75 years later.⁷ Since then, many improvements in cucurbituril synthesis, as well as in new homologue separation methods and in derivatives, have been developed by several research groups.⁸⁻¹¹

*e-mail: greg@usp.br

The general reaction based on the condensation of glycoluril derivatives and formaldehyde leads to several homologues containing mainly 5, 6, 7 and 8 glycolurilic moieties (CB[5], CB[6], CB[7] and CB[8], respectively). Among these, CB[7] is the only homologue with considerable solubility in water (*ca.* 30 mmol L⁻¹).¹² The portals are composed by carbonyl groups and behave as Pearson's hard bases. Obviously, the portal sizes vary with the number of monomeric units, ranging from 2.4 to 6.9 Å in the CB[5]-CB[8] series.^{8,12,13} Cucurbituril cavities are hydrophobic and can accommodate many guest molecules in a series of inclusion compounds, just like cyclodextrins and calixarenes (see molecular structure in Figure 1).¹¹

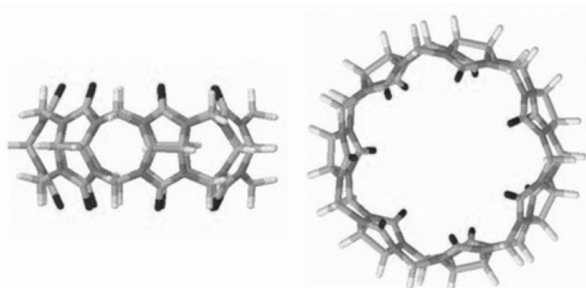


Figure 1. Representation of the chemical structure of cucurbit[7]uril.

Corma *et al.*¹⁴ have recently synthesized gold nanoparticles using CB cavities as templates, obtaining almost monodisperse particle populations, a very important aspect when one aims at absolute size control. The size control in this level is even more important during the production of quantum dots, since their physical and physicochemical properties are strongly size- and shape-dependent. According to Pearson's HSAB concept,¹⁵ Pb²⁺ ions should exhibit low affinity for cucurbiturils. However, other scientists have reported high formation constants for Pb²⁺ and decamethylcucurbit[5]uril complexes, which is a slightly different, smaller homologue.¹⁶ There are very few works in the literature reporting on CB[n]-containing nanostructured materials, but few others encompassing gold, palladium and cadmium sulfide can be cited.¹⁷⁻¹⁹

In this context, we have studied the formation of colloidal lead iodide using CB[7] acting as an external template, generating lead iodide particles with extremely reduced dimensions. We have observed the formation of randomly stacked discoid nanostructures with 1-D quantum confinement instead of small clusters.

Experimental

Cucurbit[7]uril (CB[7]) was prepared and purified as described in the literature.²⁰ Lead iodide/CB[7]

nanoparticles were prepared using Pb(NO₃)₂ 0.1 mol L⁻¹ (Synth), KI (Synth) and cucurbit[7]uril 1 × 10⁻³ mol L⁻¹. The cucurbituril solution (10 mL) was kept under vigorous stirring at 27 °C and received the addition of 100 μL of the Pb(NO₃)₂ solution, followed by 200 μL of the KI solution. The molar ratio between the reactants CB[7]/Pb²⁺/I⁻ was 1:1:2, respectively. The resulting mixture immediately formed a pale greenish-yellow colloid with gel-like consistence in a reproducible way, quite different from the large golden yellow crystals obtained when no CB[7] is present in the solution. This colloidal suspension was unstable and precipitated after two days. The resulting solid had the same greenish-yellow color and was washed three times with water (in order to remove the excess of KNO₃) and dried under vacuum. For comparison purposes, reference colloidal PbI₂ (2H-polytype) was synthesized exactly in the same way, except for the addition of the macrocycle.

The powder X-ray diffraction (XRD) measurements were carried out on a Siemens 5005 equipment using Cu K_α radiation (λ = 1.54 Å). The diffuse reflectance spectra were measured with an Ocean optics USB 4000 spectrometer at 77 K (the absorption intensities were not corrected for the powder size, which is relevant for using the Kubelka-Munk function). The luminescence experiments were registered at 77 K using a Fluorog SPEX F2121 spectrometer equipped with a 450 W Xe lamp, a cooled Hamamatsu R918 photomultiplier and double excitation and emission monochromators. The atomic force microscopy images were collected on a Shimadzu SPM-9600 scanning probe microscope (contact mode). The scanning electron microscopy and energy-dispersive X-ray spectroscopy (EDS) measurements were carried out on a Zeiss EVO 50 microscope. The samples were covered with gold by sputtering. High resolution transmission electron microscopy (HRTEM) images were obtained with a TEM-JEM 2100 ARP electron microscope. TEM sample grids were prepared by placing 1 μL of the particle suspension on a carbon-coated copper grid (300 meshes) and evaporating the solvent at room temperature.

Results and Discussion

Absorption spectra of both bulk and CB-assisted PbI₂ display typical semiconductor absorption profile, except for their typical absorption edge at *ca.* 3 eV, which is blue-shifted by 0.5 eV (*ca.* 90 nm) for the hybrid material (Figure 2). This band to band transition is frequently very close to the exciton band, since the binding energy is very small (see Supplementary Information, SI). CB[7] does not absorb in the UV-Visible region and does not contribute to the PbI₂ spectrum. It is well known that small clusters of

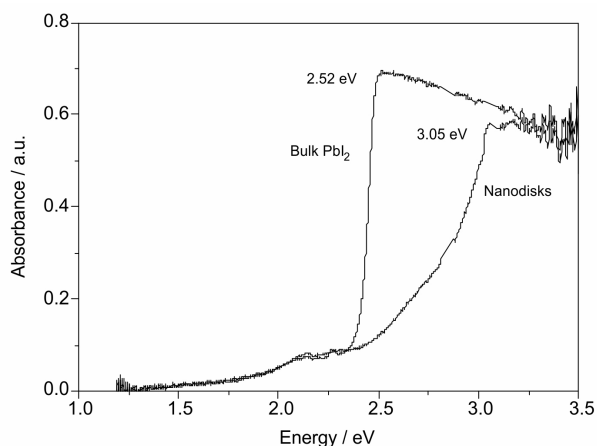


Figure 2. Absorption spectra (converted from diffuse reflectance data) of bulk PbI_2 and the CB[7]/ PbI_2 sample at 77 K.

semi-conducting materials lead to quantum confinement of excitons in one, two or three dimensions, depending on the shape and size of the particles.^{21–29} In fact, the size affects the band-gap energy when the dimension becomes inferior to the bulk-exciton Bohr radius (*ca.* 1.9 nm for PbI_2),^{21,22} although literature reveals that PbI_2 absorption edge shifts can be assigned to many other factors, from intercalation of electron-donor species between the iodide layers in few atoms clusters to ripening processes, and in low-polarity solvents.^{1,25} In fact, all these phenomena are interconnected and the shift is always related to quantum confinement mechanisms. Normally, low-polarity solvents tend to stabilize larger colloidal particles in detriment of the smaller ones as shown by Sandroff *et al.*,²⁴ but also change the dielectric constant of the medium. Small molecules can be easily intercalated into PbI_2 , once the layers are weakly held together, essentially by van der Waals interactions. The insertion of guest species between the layers has the same effect of that produced by negative pressure on this kind of lamellar material. In other words, the intercalation increases the interlamellar distances, lowering the electronic interaction between layers and the extent of the dispersion in the valence band. This increases considerably the energy, promoting 1D quantum confinement in the axial direction.²⁵

Using the effective mass approximation model, it is possible to estimate the crystallite size and thickness, as did Sandroff *et al.*²⁴ and others.^{21,22} Thus, in such anisotropic nanomaterial, the equation governing the band-gap shifts has the form:

$$\Delta E_g = \frac{\hbar^2}{2\mu_{xy}} \left[\frac{2\pi^2}{L_{xy}^2} \right] + \frac{\hbar^2}{\mu_z} \left[\frac{2\pi^2}{L_z^2} \right] \quad (1)$$

where the effective reduced masses of the electron-hole pairs in the xy plane and in the axis perpendicular to them

are represented by μ_{xy} and μ_z , respectively, and L_{xy} and L_z are the dimensions of the crystallites. The reduced masses have been experimentally determined as 0.32 (μ_{xy}) and 1.4 (μ_z) electron mass units, according to magneto-optic experiment data.^{24,30} Taking into account the absorption shift, it is reasonable to consider that almost no electronic interaction exists between the layers of PbI_2 in our case, meaning that the thickness of the nanoparticles should not be larger than a single layer of PbI_2 . When considering a single layer of the material (7 Å), equation 1 becomes:

$$\Delta E_g = \frac{235}{L_{xy}^2} + 0.55 \quad (2)$$

In our case, the shift observed is $3.10 - 2.56 \text{ eV} = 0.54 \text{ eV}$. According to equation 2, this value corresponds to the shift caused by the exfoliation of the structure, independently of the size of layers, which are too large to produce any spectral shift (the first term of such equation tends to 0 when $L_z = 7 \text{ \AA}$). Thus, the spectral shift observed for the CB[7]/ PbI_2 sample is consistent with nanoflakes constituting of PbI_2 monolayers stabilized by the macrocycle. No fluorescence at all could be measured for the hybrid solid CB[7]/ PbI_2 , indicating that the electron-hole pairs in these crystals are captured by surface traps and quenched by non-radiatively recombination processes. This is a quite common phenomenon in quantum-confined nanocrystals.^{26,31,32}

The X-ray diffraction patterns of the pure PbI_2 and CB[7]/ PbI_2 sample are compared in Figure 3. Pure PbI_2 exhibits very sharp and intense peaks characteristic of crystalline materials, while CB[7]/ PbI_2 reveals an amorphous structure, with a total loss of structural

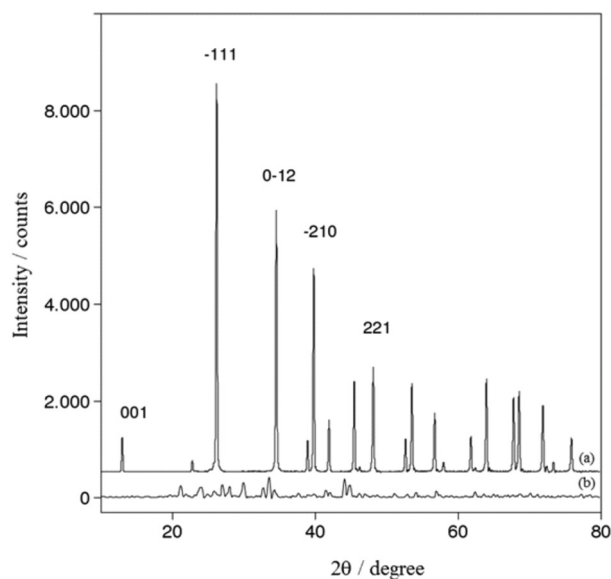


Figure 3. XRD patterns of pure PbI_2 (a) and of the CB[7]/ PbI_2 sample (b).

coherence. In fact, the absence of the 001 peak for the hybrid structure suggests the absence of a regular ordering of the PbI₂ layers and it is expected for more or less randomly-oriented isolated nanoflakes consisting of iodide monolayers. According to this, it is possible to conclude that no continuous turbostratic structure can be present, because the size of the clusters is too small for this. According to Sandroff *et al.*,²⁴ the interlayer distance of lead iodide can vary depending on the synthetic procedure, but it is never inferior to 12 Å, while the thickness of a single layer is 7 Å. The height of CB[7] molecule is 9.1 Å and should provoke an expansion of the basal distance of this magnitude if it is intercalated between the layers, acting as a pillar in the structure. An important factor that must be considered is sterical hindrance: cucurbit[7]uril is a very large molecule (*ca.* 9 Å) and it is geometrically impossible to keep a 1:1 Pb²⁺/CB[7] ratio inside a lamellar structure. Therefore, part of the macrocycle molecules would be pushed out from the structure or the iodide would be forced to adopt a crystalline configuration different from the lamellar one. Furthermore, K⁺ ions are present in large amounts in the reaction medium and it is certain that they bind the macrocycle portals, forming large cationic species in solution. These positively charged species may interact with iodine ions by electrostatic interactions, but it was verified that electron-donor species are better guests for intercalation in lead iodide. In other words, nothing favors the formation of lamellar structures in this case.³³⁻³⁸ A few and very weak signals may be observed in the diffraction pattern of the hybrid material. Even using the best acquisition methods, it is impossible to state, with our equipment, that these signals are peaks and not noise, since they are not reproducible. Furthermore, the signal does not correspond to any known PbI₂ polytype.

Medium resolution SEM micrographs (× 2,000 magnification) reveal overlaid sheets of PbI₂, just as in the case of re-crystallized matrices.³³ A SEM image obtained with high magnification (× 200,000) shows that these sheets are made of small disks measuring around 50 nm (Figure 4). EDS spectra display strong lead, iodine, carbon, oxygen and potassium signals arising from the sample (data not shown). The detected potassium is probably reminiscent from the KI starting material. This fact is easily understood once, as already mentioned, K⁺ ions form very stable coordination compounds with cucurbiturils.³⁹

The presence of the nanodisks was confirmed by AFM imaging, making clear that the sheets are composed by aggregates of regular disk-like particles. The average size was estimated to be around 34 nm (Figure 5). HRTEM images show these disks as single sheets of lead iodide that are totally exfoliated, forming a “house of cards” structure (Figure 6). This kind of structure is frequently observed in

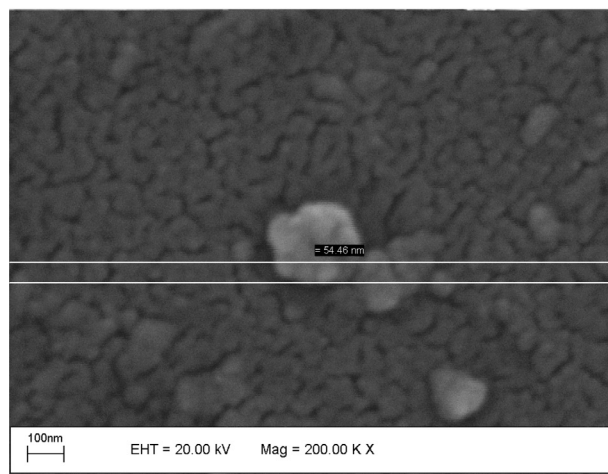


Figure 4. SEM image of the CB[7]/PbI₂ sample with aggregates under × 200,000 magnification. The grain size estimated in 54 nm.

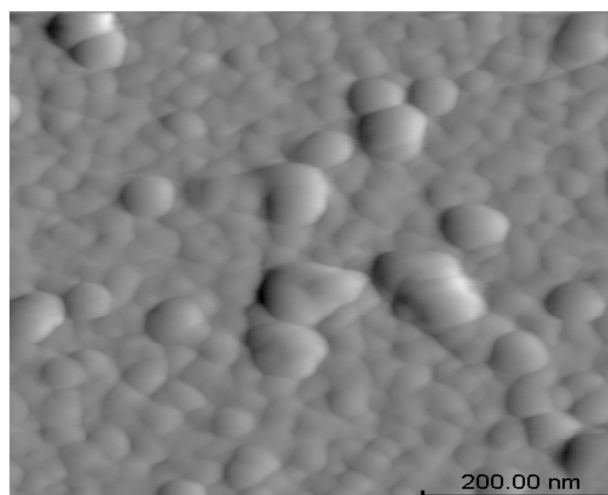


Figure 5. AFM micrograph of the CB[7]/PbI₂ sample with CB[7]/PbI₂ nanoparticle aggregates.

exfoliated clay gels, for instance Laponite[®]. In this synthetic smectite, the gel is formed by weak interactions between 1 × 25 nm disks.⁴⁰

Conclusions

CB[7] does not act as a hollow shell template for lead iodide formation as it does in the case of metal nanoparticles. The present work indicates that the macrocycle forms a random structure composed of small PbI₂ disks separated by CB[7] and K⁺ ions. The hybrid material presents reduced interlayer coupling terms, which affect its absorption spectrum when compared to pure 2H-PbI₂. The mechanism involved in the formation of this nanomaterial is complex, since it starts from an unstable colloid, which then sediments. A possible mechanism could be proposed with three major steps: the first is the formation of K₂CB[7]²⁺

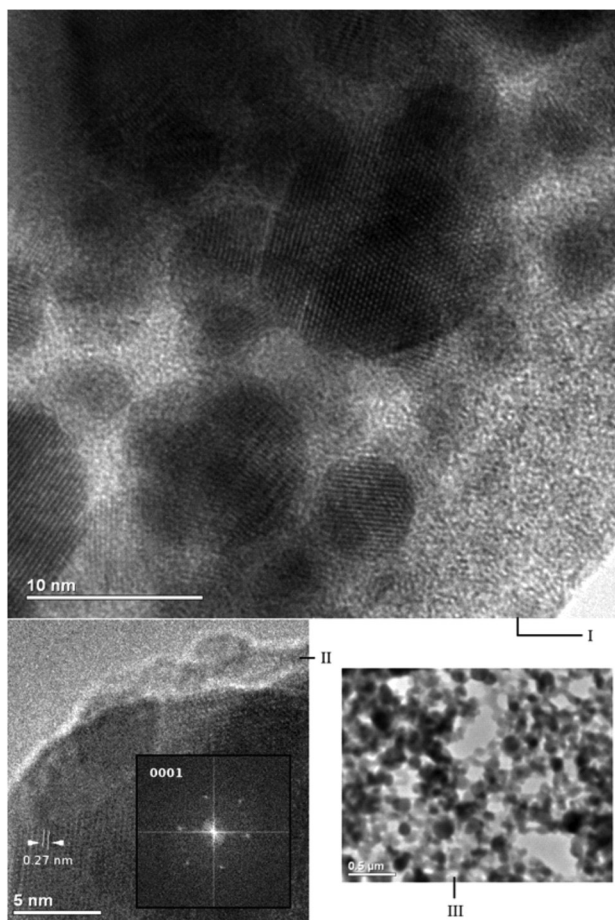


Figure 6. HRTEM micrographs of (I) the CB[7]/PbI₂ sample; (II) a single PbI₂ nanodisk (diameter *ca.* 30 nm), inset: electron diffraction pattern; and (III) CB[7]/PbI₂ sample under higher magnification, with random nanodisks in a “house of cards” arrangement.

cations which interact with iodine ions in solution. Then, lead ions bind the halogens forming nucleation centers for lead iodide single layers. As the single layers grow, CB[7] becomes too bulky and is gradually pushed to their borders, limiting nanoparticle growth. Another possibility is the formation of adducts with water molecules and Pb²⁺ ions instead of potassium complexes during the nucleation process, because this kind of structure has already been observed in many cases and with several metal ions. The nanodisk formation mechanism is still being investigated with other metal halides and will be the subject of another paper.

Supplementary Information

Additional information about the exciton band of lead iodide, including the absorption spectra of solid PbI₂ and PbI₂ nanodisks (Figure S1), is available free of charge at <http://jbcs.s bq.org.br> as PDF file.

Acknowledgements

We sincerely thank Dr. Ivana Aparecida Borin and Dr. Rodrigo Ferreira Silva for microscopy images, as well as Prof. Koiti Araki, Prof. Antonio Osvaldo Serra and Prof. Paulo César da Souza Filho for fluorescence measurements. This work was sponsored by the Conselho Nacional de Desenvolvimento Científico e Tecnológico (CNPq), Coordenação de Aperfeiçoamento de Pessoal de Nível Superior (CAPES) and Fundação de Amparo à Pesquisa do Estado de São Paulo (FAPESP). HRTEM images were obtained at Laboratório Nacional de Luz Síncrotron (LNLS, Campinas-SP, Brazil)(TEM-MS-9054).

References

1. Coleman, C. C.; Goldwhite, H.; Tikkanen, W.; *Chem. Mater.* **1998**, *10*, 2794.
2. Michalet, X.; Pinaud, F. F.; Bentolila, L. A.; Tsay, J. M.; Doose, S.; Li, J. J.; Sundaresan, G.; Wu, A. M.; Gambhir, S. S.; Weiss, S.; *Science* **2005**, *307*, 538.
3. Xu, T.; Nikiforov, A. Y.; France, R.; Thomidis, C.; Williams, A.; Moustakas, T. D.; *Phys. Status Solidi A* **2007**, *204*, 2098.
4. Tang, J.; Sargent, E. H.; *Adv. Mater.* **2010**, *20*, 1.
5. Hendrick, E.; Frey, M.; Herz, E.; Wiesner, U.; *J. Eng. Fibers Fabr.* **2010**, *5*, 21.
6. Behrend, R.; Meyer, E.; Rusche, F.; *Liebigs J.; Ann. Chem.* **1905**, *339*, 1.
7. Freeman, W. A.; Mock, W. L.; Shih, N.-Y.; *J. Am. Chem. Soc.* **1981**, *103*, 7367.
8. Day, A.; Arnold, A. P.; Blanch, R. J.; Snushall, B.; *J. Org. Chem.* **2001**, *66*, 8094.
9. Day, A. I.; Blanch, R. J.; Arnold, A. P.; Lorenzo, S.; Lewis, G. R.; Dance, I.; *Angew. Chem., Int. Ed.* **2001**, *41*, 275
10. Kim, J.; Jung, I.-S.; Kim, S.-Y.; Lee, E.; Kang, J.-K.; Sakamoto, S.; Yamaguchi, K.; Kim, K.; *J. Am. Chem. Soc.* **2000**, *122*, 540.
11. Liu, S.; Ruspic, C.; Mukhopadhyay, P.; Chakrabarti, S.; Zavalij, P. Y.; Isaacs, L.; *J. Am. Chem. Soc.* **2005**, *127*, 15959.
12. Lagona, J.; Mukhopadhyay, P.; Chakrabarti, S.; Isaacs, L.; *Angew. Chem., Int. Ed.* **2005**, *44*, 4844.
13. Demets, G. J.-F.; *Quim. Nova* **2007**, *30*, 1313.
14. Corma, A.; Garca, H.; Montes-Navajas, P.; Primo, A.; Calvino, J. J.; Trasobares, S.; *Chem. Eur. J.* **2007**, *13*, 6359.
15. Pearson, G. R.; *Inorg. Chem.* **1988**, *27*, 734.
16. Zhang, X. X.; Krakowiak, K. E.; Xue, G.; Bradshaw, J. S.; Izatt, R. M.; *Ind. Eng. Chem. Res.* **2000**, *39*, 3516.
17. Lee, T.-C.; Scherman, O. A.; *Chem. Commun.* **2010**, *46*, 2438.
18. Li, M.; Zaman, M. B.; Bardelang, D.; Wu, X.; Wang, D.; Margeson, J. C.; Leek, D. M.; Ripmeester, J. A.; Ratcliffe, C. I.; Lin, Q.; Yange, B.; Yu, K.; *Chem. Commun.* **2009**, *44*, 6807.

19. Cao, M.; Lin, J.; Yang, H.; Cao, R.; *Chem. Commun.* **2010**, *46*, 5088.
20. Day, A. I.; Arnold, A. P.; Blanch, R. J.; Snushall, B.; *J. Org. Chem.* **2001**, *66*, 8094.
21. Mallik, K.; Dhami, T. S.; *Phys. Rev. B: Condens. Matter Mater. Phys.* **1998**, *58*, 13055.
22. Finlayson, C. E.; Sazio, P. J. A.; *J. Phys. D: Appl. Phys.* **2006**, *39*, 1477.
23. Nozue, Y.; Tang, Z. K.; Goto, T.; *Solid State Commun.* **1990**, *73*, 531.
24. Sandroff, C. J.; Kelty, S. P.; Hwang, D. M.; *J. Chem. Phys.* **1986**, *85*, 5337.
25. Ghorayeb, A. M.; Coleman, C. C.; Yoffe, A. D.; *J. Phys. C: Solid State Phys.* **1984**, *17*, L715.
26. Artemyev, M. V.; Rakovich, Y. P.; Yablonski, G. P.; *J. Cryst. Growth* **1997**, *171*, 447.
27. Barnakov, Y. U.; Ito, S.; Dmitruk, I.; Tsunekawa, S.; Kasuya, A.; *Scr. Mater.* **2001**, *45*, 273.
28. Micic, O. I.; Zongguan, L.; Mills, G.; Sullivan, J. C.; Meisel, D.; *J. Phys. Chem.* **1987**, *91*, 6221.
29. Tubbs, M. R.; Forty, A. J.; *J. Phys. Chem. Solids* **1965**, *26*, 711.
30. Sandroff, C. J.; Hwang, D. M.; Chung, W. M.; *Phys. Rev. B: Condens. Matter Mater. Phys.* **1986**, *33*, 5953.
31. Dag, I.; Lifshitz, E.; *J. Phys. Chem.* **1996**, *100*, 8962.
32. Sengupta, A.; Jiang, B.; Mandal, K. C.; Zhang, J. Z.; *J. Phys. Chem. B* **1999**, *103*, 3128.
33. Schaefer, R. W.; Ardelean, M.; *Powder Diffr.* **2001**, *16*, 16.
34. Agrawal, V. K.; Chadha, G. K.; Trigunayat, G. C.; *Acta Cryst.* **1970**, *A26*, 140.
35. Chand, M.; Trigunayat, G. C.; *Acta Cryst.* **1975**, *B31*, 1222.
36. Flahaut, E.; Sloan, J.; Friedrichs, S.; Kirkland, A. I.; Coleman, K. S.; Williams, V. C.; Hanson, N.; Hutchison, J. L.; Green, M. L. H.; *Chem. Mater.* **2006**, *18*, 2059.
37. Kasi, G. K.; Dollahon, N. R.; Ahmadi, T. S.; *J. Phys. D: Appl. Phys.* **2007**, *D40*, 1778.
38. Koutselas, I.; Dimos, K.; Bourlinos, A.; Gournis, D.; Avgeropoulos, A.; Agathopoulos, S.; Karakassides, M. A.; *J. Optoelectron. Adv. Mater.* **2008**, *10*, 311.
39. Buschmann, H. J.; Cleve, E.; Schollmeyer, E.; *Inorg. Chim. Acta* **1992**, *193*, 93.
40. Kroon, M.; Vos, W. L.; Wegdam, G. H.; *Int. J. Thermophys.* **1998**, *19*, 887.

Submitted: August 21, 2010

Published online: May 24, 2011

FAPESP has sponsored the publication of this article.

Supplementary Information

Quantum Confinement in PbI₂ Nanodisks Prepared with Cucurbit[7]uril

Erick M. S. dos Santos, Lourivaldo S. Pereira and Grégoire J.-F. Demets*

DQ-FFCLRP, Departamento de Química, Universidade de São Paulo, 14040-901 Ribeirão Preto-SP, Brazil

On lead iodide exciton band

The exciton band of lead iodide does not appear always as a sharp and intense peak. Its shape and intensity may vary with crystal form, polytype, temperature, light polarization, synthetic procedure, crystallite size and especially with the purity of the material.¹ Many authors have reported similar spectra, for which the absorption edge is associated with the excitonic level, separated from gap transitions by few meV, since the binding energy is very small. The presence of electron donors in solution also affects exciton absorption bands, as demonstrated in other papers.²⁻⁵ It is well described in the literature that the first excitonic band may undergo blue shifts when extremely small particles are obtained.^{1,6-8} In the present work, a set of optical fibers and a light source essentially designed for Vis-NIR region were used in the first attempts to obtain absorption spectra. This could be the reason for the lack of spectral resolution. Furthermore, the Kubelka-Munk function could not be used since no information about the powder size of the samples after drying the colloid was known. The UV-Vis absorption measurements were repeated at room temperature (Figure S1), using another set of optical fibers designed for working in the UV region. This time the bands clearly appear. Using the Tauc equation, the E_g value was calculated, being 2.34 and 2.80 eV (diff = 0.46 eV) for bulk PbI₂ and the nanodisks, respectively.

For pure lead iodide, the exciton band is located at the absorption edge (499 nm), which is coherent with the literature (490-500 nm). For the nanodisks, it is blue-shifted to 387 nm and a small shoulder is observable at 499 nm, which could be assigned to larger aggregates or to heteronuclear excitons.³ As mentioned before, these new values were obtained at room temperature, but the onset absorption energies do not vary considerably from our previous measurements at 77 K (see Figure 2 in the main text), and would not affect the presented conclusions from the effective mass model. Probably, the problem is related to our experimental apparatus.

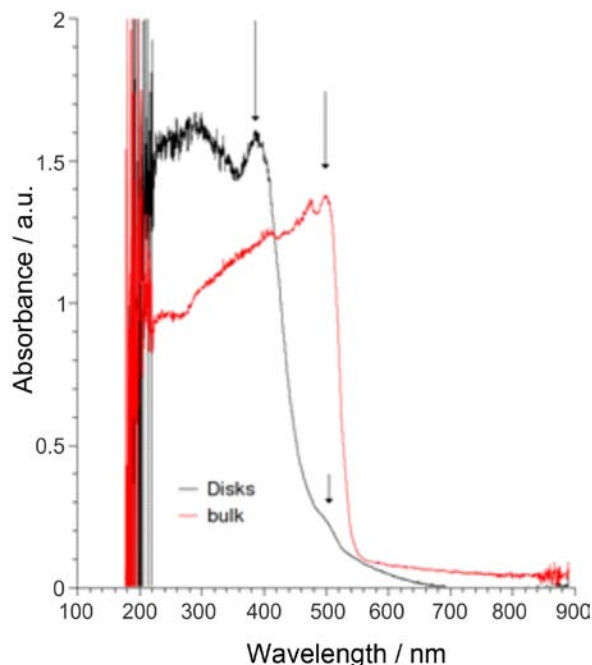


Figure S1. Absorption spectra of solid PbI₂ and PbI₂ nanodisks at room temperature.

References

1. Tubbs, M. R.; Forty, A. J.; *J. Phys. Chem. Sol.* **1965**, *26*, 711. (29 in the Article text).
2. Sengupta, A.; Jiang, B.; Mandal, K. C.; Zhang, J. Z.; *J. Phys. Chem. B* **1999**, *103*, 3128. (32 in the Article text).
3. Bhavsar, D. S.; Saraf, K. B.; *J. Mater. Sci.: Mater Electron.* **2003**, *14*, 195.
4. Koutselas, I.; Dimos, K.; Bourlinos, A.; Gournis, D.; Avgeropoulos, A.; Agathopoulos, S.; Karakassides, M. A.; *J. Optoelectron. Adv. Mat.* **2008**, *10*, 311.
5. Nozue, Y.; Tang, Z. K.; Goto, T.; *Solid State Commun.* **1990**, *73*, 531. (23 in the Article text).
6. Kasi, G. K.; Dollahon, N. R.; Ahmadi, T. S.; *J. Phys. D: Appl. Phys.* **2007**, *40*, 1778. (37 in the Article text).
7. Artemyev, M. V.; Rakovich, Y. P.; Yablonski, G. P.; *J. Cryst. Growth* **1997**, *171*, 447. (26 in the Article text).
8. Micic, O. I.; Li, Z.; Mills, G.; Sullivan, J. C.; Meisel, D.; *J. Phys. Chem.* **1987**, *91*, 6221.

*e-mail: greg@usp.br